

A 2-D AXISYMMETRIC GAS FLOW MODEL

Marek Gono

*Slovak University of Technology, Faculty of Mechanical Engineering, Department of Automobiles,
Combustion Engines and Ships
Nam. slobody 17, 81231 Bratislava, Slovakia
tel.: +421 2 572 96 400, fax: +421 2 52 96 26 50
e-mail: marek.gono@stuba.sk*

Richard Pearson

*Lotus Engineering
Potash Lane, Hethel, NR14 8EZ, United Kingdom
tel. +44 1953 608 683, fax: +44 1953 608 157
e-mail: rpearson@lotuscars.co.uk*

Marian Poloni

*Slovak University of Technology, Faculty of Mechanical Engineering, Department of Automobiles,
Combustion Engines and Ships
Nam. slobody 17, 81231 Bratislava, Slovakia
tel.: +421 2 572 96 300, fax: +421 2 52 96 26 50
e-mail: marian.poloni@stuba.sk*

Abstract

A 2D axisymmetric unsteady flow model is to be developed and integrated with a 1D engine cycle simulation code. The model assumes inviscid flow and is supposed to be capable of accurate modelling of various manifold elements like bell-mouth entry or catalyst entry diffuser and exit effuser. Rapid runtime and ease of meshing are of absolute importance. A finite volume mesher was developed and is capable of rapid meshing of variable area ducts as well as of their external region. The 2D planar and 2D axisymmetric MacCormack solvers were constructed and tested in straight- and diverging pipe shock tube tests. A non-reflecting boundary condition was applied to the border of the computational domain in order to prevent wave reflections from this non-physical boundary. The shock-tube test results were compared against those from the quasi-1D MacCormack and first order HLLC solvers. The MacCormack method, used without flux limiter, was found to be too dispersive and unable to represent the reality at required precision level. Consequently it was decided to develop a brand new solver that will employ the modern and robust Hancock MUSCL scheme.

Keywords: *engine manifold design, unsteady gas flow, variable cross section duct*

1. Introduction

Today, 1D engine cycle and gas dynamics simulation codes are widely used tools in the design of piston combustion engines. They are characterized by an outstanding combination of rapid runtime and relatively high precision of results; thanks to the combination of a 1D gas dynamic model in the manifold and 0D solving approach to all other elements (cylinders, turbochargers, plenums, etc.). Typical applications of these codes include prediction of performance parameters, manifold tuning, valve and ignition timing optimization, turbocharger matching etc. These codes solve the so-called Euler equations - with modifications to account for the effects of pipe wall

friction, heat transfer, and pipe area variation - in order to obtain time-dependent state parameters of the unsteady gas flow throughout the manifold at defined engine speed and load conditions. These equations are a set of three conservation laws (continuity, momentum and energy equations) of inviscid flow. Though the codes take into account the phenomena of friction, heat transfer or even chemical reactions, they sometimes exhibit serious troubles when a user attempts to build a high-fidelity (from the point of view of geometry features) model of real manifold system. Features like bends, junctions, or plenums can be solved fairly well with one of the established methods [2]. On the other hand, tapered ducts (which are abundant features in engine manifold systems) are supposed to obey the quasi-1D formulation of equations stating that the flow always adheres to the walls and radial flow effects can be neglected. This is true for slight area variations (up to approximately 7-10°) and weak disturbances only; when the area variation is larger and/or flow velocity higher and/or discontinuities are present, this assumption is completely invalid and the calculation error may reach 40% [4]. At even greater area changes the code is likely to crash due to instability of employed numerical scheme [2]. In such a case the only way, in which the model is solvable, is to turn the gradual taper into sudden area change and apply an appropriate boundary condition. However, the boundary condition for a sudden area change is based on the simplified assumption of the flow fully separating the walls; and this is also not an accurate representation of the system. A remedy to the above-mentioned issues has been proposed by Corberan et. al. [1]. It is based on a modified interpretation of governing equations and modified meshing approach. When combined with classical two-step Lax-Wendroff method or TVD-class Roe-solver-based numerical scheme, it results in extremely stable technique able to successfully solve even very large taper angles while low runtime costs is maintained. However, this does not completely resolve the issue that the real flow will separate from the pipe walls, in which case the fluid velocity becomes decoupled from the pressure over part of the pipe cross-section. An alternative to Corberan's approach is to rely on a link to a commercial 3D CFD package that solves the flow in the critical part. Though the results obtained can be very accurate if the coupling is properly performed, a major disadvantage of these coupled simulations lie in the significant increment of calculation runtime. Additionally, the users are required to be licensed for the use of the CFD software they may not need for anything else - this is likely to be economically unviable for many of the 1D code users. The ideal solution seems to be the integration of a multi-D gas flow sub-model into a 1D simulation code; such that the user can control the compromise in accuracy and runtime increase. Ideally, this sub-model would be based on a full 3D solver; this would, on the other hand, require a sophisticated mesh tool and skilled CFD simulation engineer. A 2D planar model is valid exactly only for rectangular cross sections as it assumes a unit width at all nodal points. Thus, the logical compromise is a 2D axisymmetric model.

2. 2D axisymmetric flow model

The symbolic vector equation governing 2D axisymmetric gas flow can be written as [3,4]

$$\frac{\partial W}{\partial t} + \frac{\partial F}{\partial x} + \frac{\partial G}{\partial y} + \frac{1}{y} \cdot R = 0 \quad , \quad (1)$$

where state vector, flow vectors, and 'radial' vectors are given by

$$W = \begin{pmatrix} \rho \\ \rho \cdot u \\ \rho \cdot v \\ \rho \cdot e_0 \end{pmatrix}; \quad F = \begin{pmatrix} \rho \cdot u \\ \rho \cdot u^2 + p \\ \rho \cdot u \cdot v \\ \rho \cdot u \cdot h_0 \end{pmatrix}; \quad G = \begin{pmatrix} \rho \cdot v \\ \rho \cdot u \cdot v \\ \rho \cdot v^2 + p \\ \rho \cdot v \cdot h_0 \end{pmatrix} \quad \text{and} \quad R = \begin{pmatrix} \rho \cdot v \\ \rho \cdot u \cdot v \\ \rho \cdot v^2 \\ \rho \cdot v \cdot h_0 \end{pmatrix}.$$

Note that in this form the equation neglects the friction, heat transfer and chemical reactions; but the extension to such a form is straightforward. This is a typical set of hyperbolic first-order partial

differential equations and can be solved by any of classical or more modern shock-capturing numerical schemes.

While finite difference discretization defines the calculation points, the finite volume discretization defines the borders of the control volume (calculation cell) and is therefore independent of cell geometry. Thus, the requirement of ease of meshing and extensibility to more complex features is better satisfied by FVM discretization. The mesh generation code was programmed in the Fortran 95 programming language and is capable of meshing the interior and exterior of a given variable-cross section duct. The exterior around the pipe exit/entry is to be meshed and solved in order to correctly capture the end effect (i.e. wave reflection slightly beyond the exit rather than directly at the end of the duct). The dimensions of meshed external region (green, turquoise and violet mesh) can be seen in the Fig. 1.

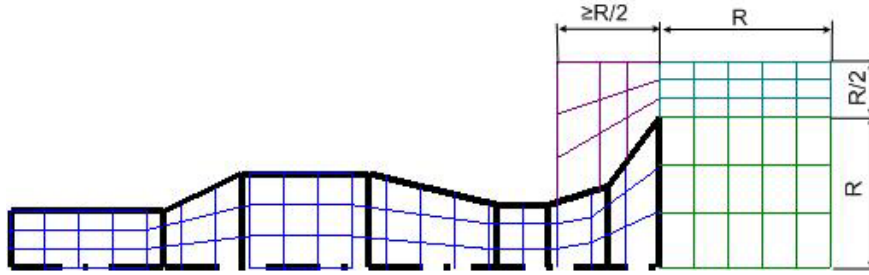


Fig. 1: The example of computational mesh of a variable cross-section duct

Along with the mesh generator, the cell-centred FVM solver utilizing the well-known MacCormack predictor-corrector method was programmed. This method is summarised as [3]:

$$W_i^{\text{pred}} = W_i^n - \frac{\Delta t}{\Omega} \cdot (F_{i+1}^n - F_i^n + G_{i+1}^n - G_i^n) - \frac{\Delta t}{y_{CG}} \cdot R_i^n,$$

$$W_i^{\text{cor}} = W_i^n - \frac{\Delta t}{\Omega} \cdot (F_i^n - F_{i-1}^n + G_i^n - G_{i-1}^n) - \frac{\Delta t}{y_{CG}} \cdot R_i^n, W_i^{n+1} = \frac{1}{2} \cdot (W_i^{\text{pred}} + W_i^{\text{cor}}) \quad (2)$$

The MacCormack scheme was not actually expected to fulfil the stability and precision requirements as, being a linear scheme of second-order accuracy, it does not satisfy the TVD criterion. At this early stage of the code development it was employed mainly for its simplicity and ease of programming such that quick comparisons of 2D planar and 2D axisymmetrical approaches could be made, together with verification of various combinations of boundary conditions. These analyses, as well as the overall behaviour of the model were studied with a standard constant area shock-tube test (Sod's problem) as well as a non-standard variable cross-section shock-tube test, similar to the de Haller test. Actually, the codes were tested for shock-tube and de Haller behaviour with converging and diverging tubes and a convergent-divergent nozzle, but due to limited space only the former two tests are presented here.

Along with solving equation (2), the solver works with boundary conditions (BCs). A simple no-slip ($u=v=0$) BC was applied to solid walls of the pipe. The "inlet" BC (left end of the pipe) was defined by a prescribed value of pressure, $p=p_2$. The centreline BC suppresses the radial velocity ($v=0$) while maintaining the value of the axial velocity u . Simple "outlet" BC prescribing the value of pressure p_1 causes waves to reflect at the border of the computational domain. These reflections distort the calculation, as the domain boundary is only virtual and does not exist in reality. To address this issue a non-reflecting boundary condition (NRBC), based on the simple mirror image assumption of the ghost cell [5], was introduced. The domain boundary treated with this kind of boundary condition absorbs waves well and eliminates distortions of this type from the

calculation. The relationship between the last internal cell, P , and the ghost cell, Q , for a simple NRBC is given by $W_P^n = W_Q^n$.

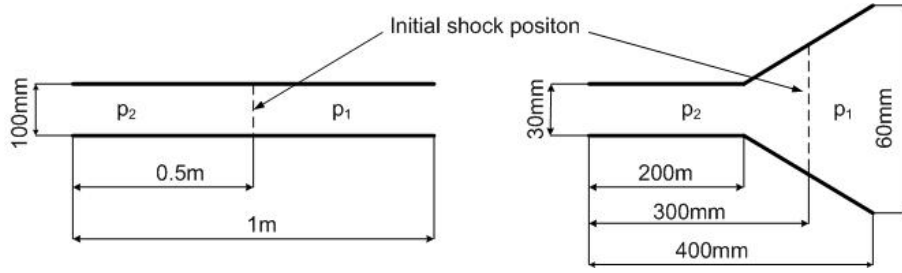


Fig. 2: Dimensions of tubes for Sod's problem: straight pipe on the left and variable cross-section pipe on the right

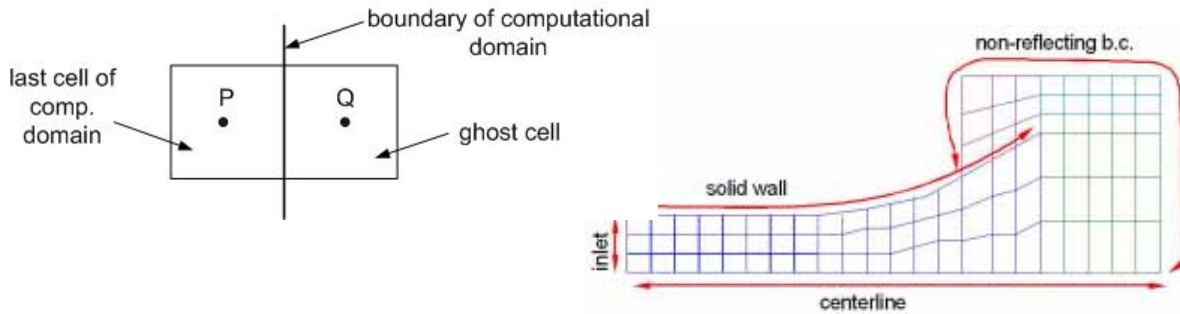


Fig. 3: Non-reflecting BC - mirror image assumption (left) and boundary conditions applied to tested tube (right)

Straight- and diverging pipe shock-tube tests were performed with both 2D planar and 2D axisymmetric MacCormack solvers. The initial conditions of the test were: $p_1=100$ kPa, $p_2=130$ kPa, $T_1=T_2=300$ K and $u_1=v_1=u_2=v_2=0$. The dimensions of the pipes and the initial position of the shock are shown in the Fig. 2. The straight pipe was divided into 200 axial and 40 radial meshes (30 in the axisymmetric case); the variable cross-section pipe was meshed into 200 axial and 30 radial meshes (in both planar and axisymmetric case).

3. Test results

It should be noted that in the case of straight pipe the external regions were meshed at both pipe ends (Figs. 4 and 5; the pipe geometry is outlined by black lines) and that NRBC was applied to the border of the computational domain in order to prevent wave reflections and calculation distortion. When solving the Sod's problem in the straight pipe using 2D planar approach, the MacCormack solver crashed after approx. 12.8 ms of runtime due to numerical overshoots in the vicinity of the sudden area change (pipe end – outflow region interface). Small dark blue spot can be observed at the right end of the pipe in Fig. 4: this marks the location with very low value of calculated pressure that leads to a zero and, eventually, a negative value of density – and this causes the code to crash. The red spot, i.e. high-pressure region, just next to low-pressure region, gives a further indication of a physically impossible situation.

Using the 2D axisymmetric approach, the MacCormack solver crashed after approx. 3.75 ms of runtime again due to numerical overshoots in the vicinity of the sudden area change. Non-physical oscillations of pressure (red and orange stripes) can be seen at the left end of the pipe in Fig. 5. As well, dark blue spots in the upper section of the left pipe's end mark the locations with very low

value of calculated pressure that leads to zero and eventually negative values of density and causes the code to crash.

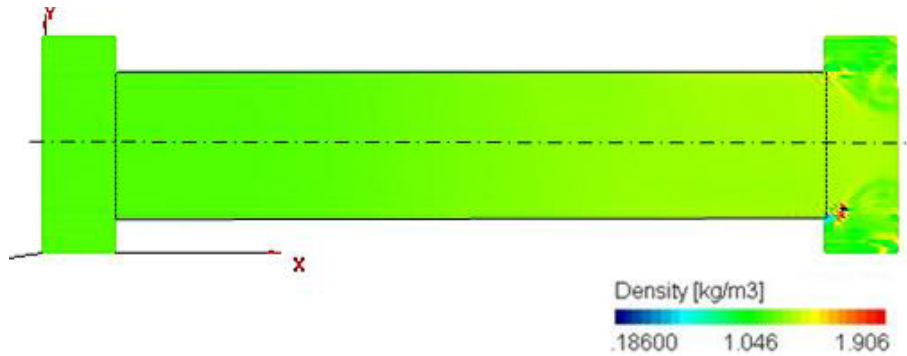


Fig. 4: Density contours in the straight-pipe shock tube test after 12.8 ms, 2D planar case

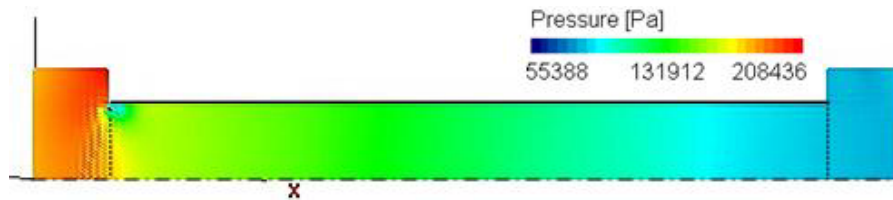


Fig. 5: Pressure contours in the straight-pipe shock-tube test after 3.75 ms, 2D axisymmetric case

The “bell-mouth entry shock-tube test” was performed with variable cross-section pipe (Fig. 2 right) with meshed external region on the right hand side. The initial conditions were as above. In Fig. 6 one can observe nice patterns of flow separation (orange and yellow-to-green stripes along the tapered section of the duct) as well as the absorbance of incident wave by the NRBC of the computational domain. However, the tiny small blue spot right at the transition of the straight pipe into a taper is of the main interest in this figure. It marks the location with low density that in the very next time step falls below zero and causes the code to crash (after approx. 4.25 ms).

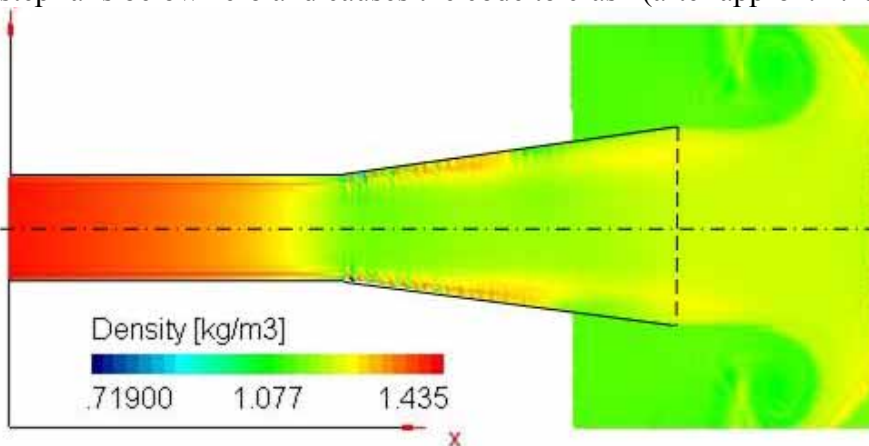


Fig. 6: Density contours in and around bell-mouth entry after 4.25 ms, 2D planar case

Fig. 7 presents pressure contours in the bell-mouth entry solved as a 2D axisymmetric case for approximately 2.9 ms. A strange pressure pattern in the bottom right corner can be seen (zoomed in dotted region) - these numerical oscillations eventually grow up to such an extent that they cause the code to crash due to a negative value of calculated density. This kind of oscillation is

believed to be a result of a combination of centreline B.C. and mirror-image-based NRBC. However, this particular case crashed due to negative density calculated at the area change in the middle of pipe (small blue dot). Approximately 30 different geometries of variable area ducts were tested at equal initial conditions while different combinations of boundary conditions were applied to the centreline and domain border. It has been found that, in general, calculations of bell-mouth entries with larger taper angles tend to crash due to negative density at the area change inside the pipe while calculations of slimmer “trumpets” crash due to oscillations along centreline arising from the NRBC in the bottom right corner. However, this general rule varies with mesh size. The size of the meshed external region around the pipe exit/entry played no role in the development of this kind of oscillations.

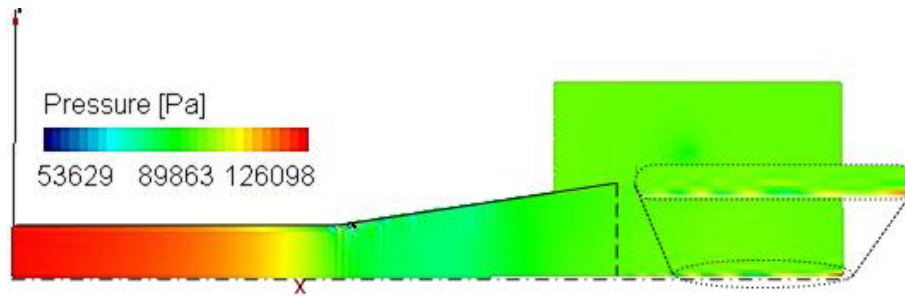


Fig. 7: Pressure contours in and around bell-mouth entry after 2.9ms

It should be noted that similar situation was observed when certain combinations of shock strength, boundary conditions, mesh size and external region size were applied to the 2D axisymmetric straight pipe shock-tube test. Fig. 8 shows an example of 2D axisymmetric straight pipe shock tube test with NRBC applied to both its ends – the oscillations start to develop at approx. 8 ms in the left portion of the pipe, continue to grow up and cause the calculation to crash after 13 ms.

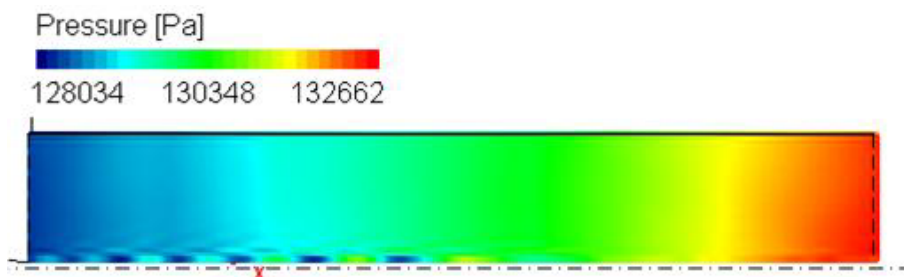


Fig. 8: Pressure contours in the straight pipe shock tube test after 11ms

When comparing straight-pipe shock-tube test results provided by 2D planar and 2D axisymmetric MacCormack solvers with those obtained through quasi-1D MacCormack and 1st order HLLC solvers, shown in Fig. 9a, it can be seen that though both 2D planar and 2D axisymmetric solvers predict the shock position relatively well, they produce numerical overshoots of notable similarity. However, after a certain runtime value is reached, the calculated pressure traces differ more and more: as the 2D planar approach is somewhat more stable, it gives slightly smoother curves, whereas the 2D axisymmetric approach suffers from spurious oscillation from early runtimes. When a diverging pipe (uniform diameter change from 200mm to 400mm on 1m of length) was subjected to the above-described shock-tube test, the results were found to be somewhat similar to

those from straight pipe, as far as the overall form of the curves is considered, Fig. 9b. Naturally, the results from 1D and 2D approaches differ more.

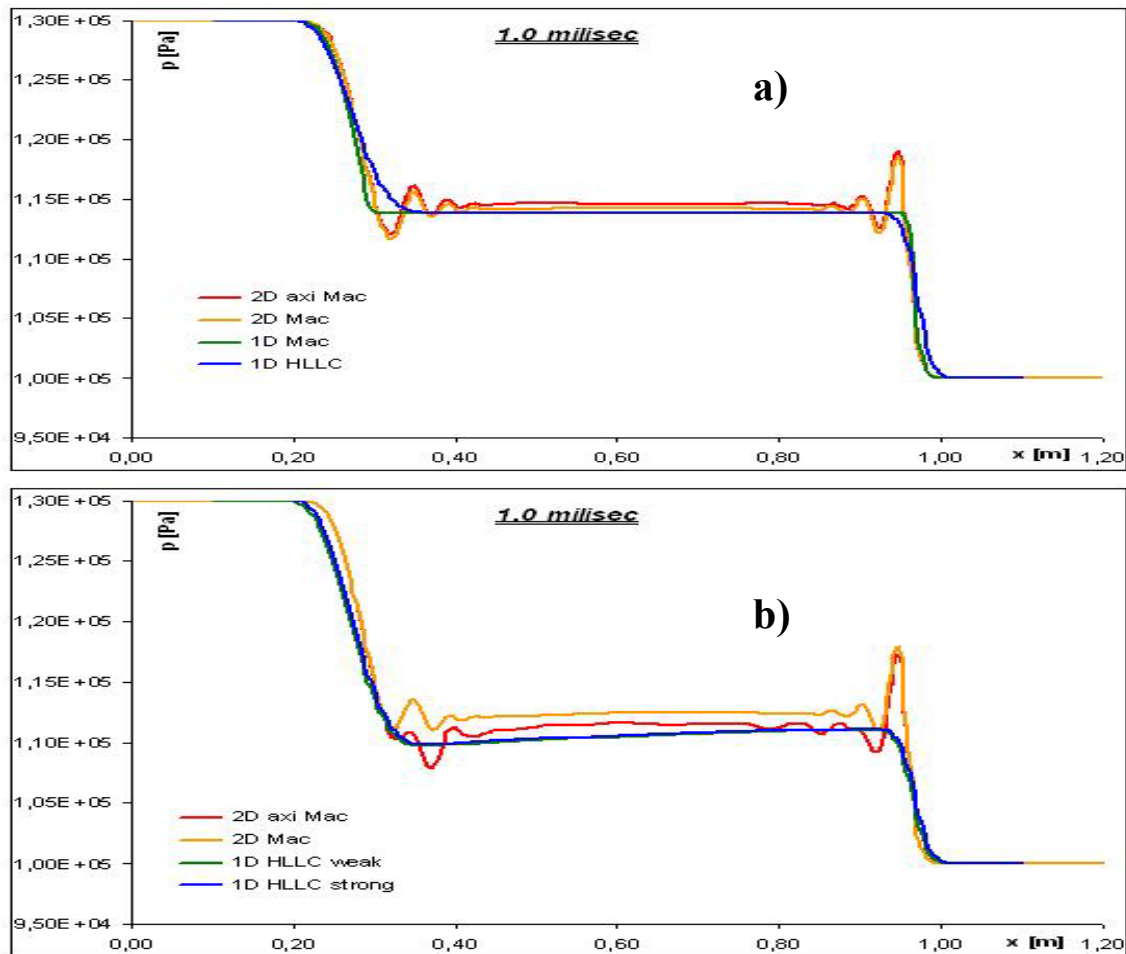


Fig. 9: Centreline pressure traces in a) straight- and b) diverging pipe shock-tube test.

3. Conclusion

The MacCormack method was found to be too dispersive and unstable to be usable in the 2D axisymmetric flow submodel. The application of a flux limiter to the above-described combination of the flow model and numerical method would significantly improve the predictions but it is thought the development of a brand new solver based on a more recent numerical technique is preferable. This will employ a modern robust numerical method, namely the Hancock MUSCL scheme, which provides high-resolution oscillation-free results whilst the runtime cost increment is insignificant. Another conclusion to be drawn is that the non-reflecting (absorbing) boundary condition, even in its simplest form of mirror-image ghost cell, performs much better than ordinary outlet BC that assigns a value of pressure to particular cell boundary. The incident waves are absorbed by NRBC rather than being reflected back straightaway; the reality is modelled in more accurate way. However, certain attention is to be paid to specific combination of boundary conditions in order to prevent distorted results as described above.

Acknowledgement

The research at the Department of Automobiles, Combustion Engines and Ships is supported by the VEGA 1/3171/2006 grant project of the Ministry of Education of the Slovak Republic.



The presented research project was supported by the ESF project JPD3 2004/1-032 code 131 202 000 24.

We would like to thank the directors of Lotus Engineering for hosting the primary author during the course of this study.

Nomenclature

e_0 - total stagnation internal energy, F - flux vector, FVM - finite volume method, G - flux vector, h_0 - total stagnation enthalpy, HLLC - Harten - Lax - van Leer contact wave solver, MUSCL - monotonic upwind scheme for conservation laws, p - pressure, R - radial term or pipe radius, TVD - total variation diminishing, u - axial velocity, v - radial velocity, W - state vector, y_{CG} - radial coordinate of gravity centre, ρ - density

References

- [1] Corberán, J.M., Gascón, Ll.: *New method to calculate unsteady 1D compressible flow in pipes with variable cross section*, ICE vol. 23, Engine Modelling ASME conference, 1995.
- [2] Gono, M.: *Unsteady gas flow in combustion engine manifold* (in Slovak), research report, KALSM Sjf STU Bratislava, 2006.
- [3] Hirsh, C.: *Numerical computation of internal and external flows, vol. 2: Computational methods for inviscid and viscous flows*, J.Wiley & sons, 1990.
- [4] Igra, O., Wang, L., Falcovitz, J.: *Non-stationary compressible flow in ducts with varying cross-section*, Proc. Instn, Mech. Engrs. vol. 212 part G.
- [5] Loh, C.Y.: *On a non-reflecting boundary conditions for hyperbolic conservation laws*, NASA/CR-2003-212387 paper.